

41st Danubia-Adria Symposium Advances in Experimental Mechanics September 23-26, 2025, Kragujevac, Serbia



Extended abstract DOI: <u>10.46793/41DAS2025.041L</u>

ANALYSIS OF TEST STRAIN IN A FOUR-POINT BENDING CALIBRATION SETUP FOR STRAIN GAGES

Thomas Lehmann¹, Tobias Jähnichen², Jörn Ihlemann³

- ¹ <u>0000-0001-7887-6772</u>, Chemnitz University of Technology, Chair of Solid Mechanics, Reichenhainer Str. 70, 09126 Chemnitz, Germany, E-mail: thomas.lehmann@mb.tu-chemnitz.de;
- Chemnitz University of Technology, Chair of Solid Mechanics, Reichenhainer Str. 70, 09126 Chemnitz, Germany;
- ³ <u>0000-0002-3831-0712</u>, Chemnitz University of Technology, Chair of Solid Mechanics, Reichenhainer Str. 70, 09126 Chemnitz, Germany, E-mail: joern.ihlemann@mb.tu-chemnitz.de

1. Introduction

Strain analysis is of particular importance in experimental mechanics. For the measurement of very small strains, strain gages are often used due to their outstanding precision and accuracy. Thus, the calibration of strain gages (gage determination) is to be done considering high requirements [1]. Therefore, a four-point bending setup is suitable due to the clear defined strain distribution in the analyzing section, where the strain gages are applied [2]. The determination of the test strain is of particular importance here. In this contribution, two different measurement methods using displacement transducers and 3D digital image correlation (DIC) - are applied for the determination of the test strain and compared. The DIC strain evaluation used here deviates from the method based on spline approximation of the displacements or coordinates, given, e. g., in [3].

2. Experimental setup and procedure

The test setup includes a four-point bending loading device, following [1], cf. Fig. 1. The force F is applied by a load application traverse and rollers to the specimen, which is designed as a narrow bending beam, made of aluminum (EN AW- $6082, 20 \times 20 \times 320, w \times h \times l$ in mm). Furthermore, the specimen is supported by rollers, which are connected to a supporting structure. The four-point bending device is implemented in a 100 kN ZwickRoell testing machine. Four strain gages (two at the top, two at the bottom) of the type HBM/HBK 1-LY43-6/350 are applied in the analyzing section between the load application. Incremental displacement transducers (Heidenhain MT2571, contact measuring system) and a 3D DIC system (GOM Aramis 4M, adequate speckle pattern and measuring volume required) are used for the

determination of the test strain ε_t in x-direction. Loading is carried out with a traverse speed of 1 mm/min and a maximum force $F_{\text{max}} \approx 3 \text{ kN}$.

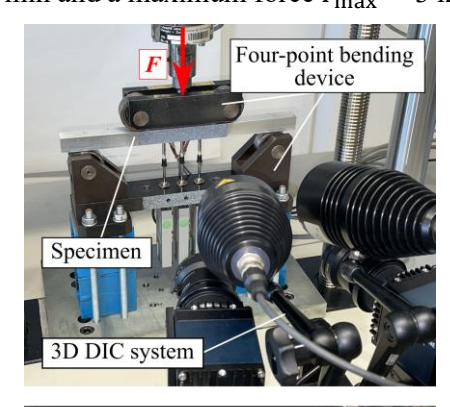




Fig. 1. Four-point bending test setup.

3. Strain and gage factor determination

Based on the constant curvature (circle arc) in pure bending, the test strain ε_t at the bottom side of the specimen is determined taking into account the height h, the distance between the displacement transducer tips a and the averaged deflection (displacement) differences p, cf. Fig. 2:

$$\varepsilon_{x\,t} = \varepsilon_t = \frac{h}{\frac{a^2}{n} + p - h} \tag{1}$$

Furthermore, using DIC, the test strain is calculated by approximating the DIC displacement data u_y with a circular arc fit. Using the resulting curvature radius ρ , the strain ε_x on the front and the test strain ε_t at the bottom side are defined by:



41st Danubia-Adria Symposium Advances in Experimental Mechanics September 23-26, 2025, Kragujevac, Serbia





$$\varepsilon_x(y) = -\frac{y}{\rho(y)+y} \rightarrow \varepsilon_{x\,t} = \varepsilon_t = \frac{h}{2[\rho(y)+y]}.$$
 (2)

Additionally, on the basis of ε_t and the bridge output $V_{\rm out}/V_{\rm in}$ (quarter bridge), the gage factor k is determined, cf. Eq. (3). The relative gage factor deviation $\Delta k/k_0$ (relative deviation of the determined gage factor from the value of the data sheet $k_0 = 2.11$) is then calculated by:

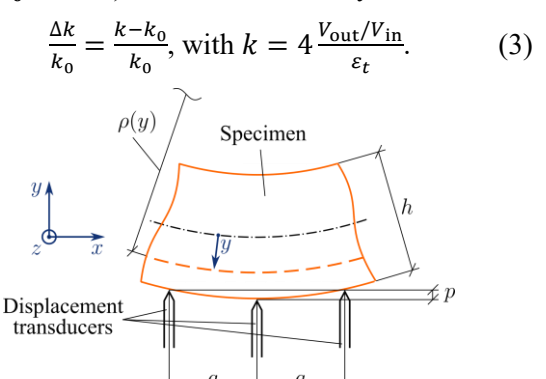


Fig. 2. Bending deformation, test strain determination.

4. Results

In the strain vs. force diagram for a representative test example shown in Fig. 3, good agreement of the strain results at the bottom of the specimen using the different methods is demonstrated (ε_t by displacement transducers, DIC; ε_{SG} by strain gages using k_0 – averaged for the two strain gages at the bottom).

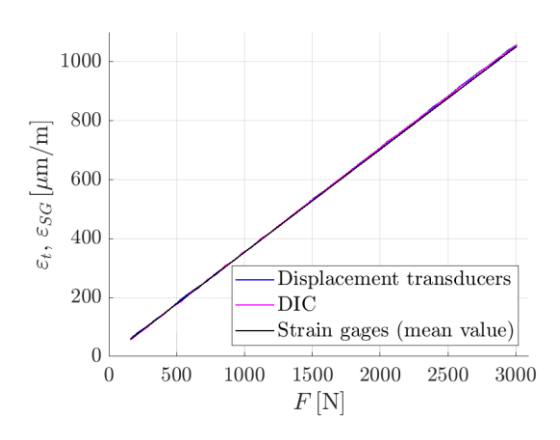
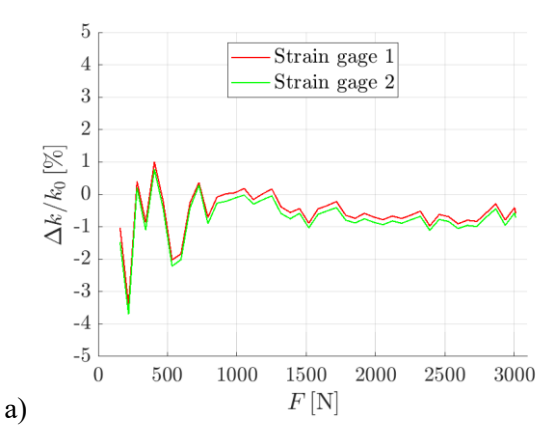


Fig. 3. Strains vs. force *F* using different methods for strain determination.

This is also directly reflected in the gage factor results. In Fig. 4, the relative gage factor deviation vs. the force is shown for the test example using the methods presented. Good agreement between the test strain determination methods with maximum deviations of $|\Delta k/k_0| \approx 1$ % is observed at the higher loads (> 800 N). Furthermore, very good matching of both strain gage signals is demonstrated. Test series have shown, that good

displacement transducer results are only achieved, as long as the surface quality of the contact area is high (disadvantage of the contact to the specimen).



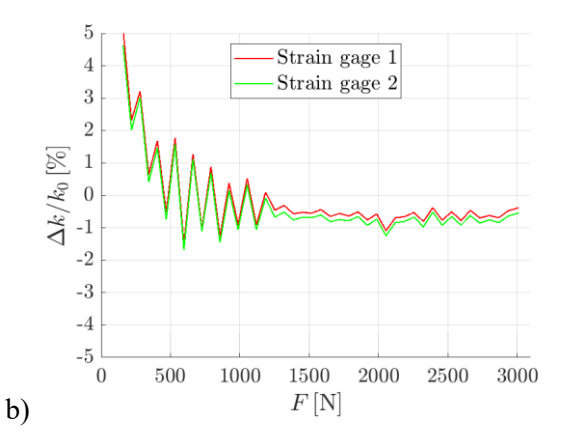


Fig. 4. Relative gage factor deviation $\Delta k/k_0$ vs. force F, a) based on displacement transducers, b) based on DIC.

5. Conclusions

Precise strain analyses were carried out in a fourpoint bending calibration test setup for strain gages. The determined test strains using displacement transducers and 3D DIC show good agreement between the two methods and with the strain gage values (using k_0). Thus, good results are obtained for the gage factor (with limitations using displacement transducers) demonstrated by small relative deviations from the data sheet value, which are within the tolerance range of the strain gages.

References

- [1] VDI/VDE standard 2635-1. Experimental structure analysis Metallic bonded resistance strain gauges Characteristics and testing conditions, 2024.
- [2] Bergqvist, B. Equipment for highly accurate and repeatable strain gauge factor determination. *Strain*, 1972, 8(4), 170–176.
- [3] Lehmann, T., Ihlemann, J. DIC deformation analysis using B-spline smoothing with consideration of characteristic noise properties. *Mater Today-Proc*, 2022, 62(5), 2549–2553.